This is a repository copy of *Determination of the origin of anomalous eutectic structures from in-situ observation of recalescence behaviour*.

White Rose Research Online URL for this paper:
http://eprints.whiterose.ac.uk/79859/

Determination of the Origin of Anomalous Eutectic Structures from In-situ Observation of Recalescence Behaviour

Andrew M Mullis[1,a], Caroline R Clopet[1,b] and Robert F Cochrane[1,c]

[1]Institute for Materials Research, University of Leeds, Leeds, LS2-9JT, UK.

[a]a.m.mullis@leeds.ac.uk, [b]c.r.clopet05@leeds.ac.uk, [c]r.f.cochrane@leeds.ac.uk

Abstract. A melt encasement (fluxing) method has been used to undercool Ag-Cu alloy at its eutectic composition. The recalescence of the undercooled alloy has been filmed at high frame rate. At low undercooling lamellar eutectic is observed to grow, giving way to a mixed anomalous-lamellar structure at higher undercooling. *In situ* observation of the spot brightness reveals, as expected, that the lamellar eutectic grows via a planar front mechanism, while the anomalous eutectic grows via a more complex process characterised by a double recalescence. The first recalescence is non-space-filling (dendritic) in character and is followed shortly afterwards by a second recalescence which appears to be of the planar front type. Moreover, the first recalescence event appears to be to a temperature in excess of the equilibrium eutectic temperature. This is strongly suggestive that the anomalous eutectic morphology arises due to the growth and subsequent partial remelting of a dendritic morphology, probably a two-phase (eutectic) dendrite, followed by planar front growth of a lamellar eutectic into the residual liquid.

Introduction

With increasing departures from equilibrium a number of morphological changes are observed during the growth of eutectic alloys. In particular, as the liquid is progressively undercooled a number of systems, including Ni-Sn [1, 2], Ni-Si [3, 4], Co-Sn [4] and Ag-Cu [5, 6], have been reported to display a transition from a regular lamellar to an anomalous eutectic structure. In most cases this is a progressive transition, with increasing volume fractions of the anomalous eutectic being formed as the undercooling is increased. For such materials with a mixed lamellar/anomalous eutectic structure, such as Ag-Cu at low undercooling, it has been suggested that the anomalous structure is a direct product of rapid solidification, forming first with the eutectic lamellae growing slowly after the initial recalescence event [5].

In the sense used here we define the formation of anomalous eutectic as indicating a transition from a regular lamellar structure to one which although still two phase is more globular in nature, sometimes exhibiting a swirled or random mixing of the phases and which is generally much coarser than the equivalent lamellar structure, with which it coexists. This should be distinguished from an alternative use of the term anomalous eutectic, which indicates a structure which is still lamellar, but in which the lamellar spacing deviates significantly from the extremum spacing as one or both phases show a strong preferential growth direction. Although this gives rise to some potential for confusion, the anomalous eutectic terminology has been used to describe both morphologies for a significant period and we do not here attempt to correct this historical anomaly.

There has been much debate on the formation mechanism of anomalous eutectics. Suggestions for the mechanism have included the decomposition of a dendritic supersaturated single-phase solid-solution [1], decoupled growth of the lamellar eutectic [4, 7], fragmentation or remelting of primary lamellar eutectics [3, 6] and remelting of eutectic dendrites [8]. The issue has been clarified somewhat by the recent work of Yang *et al.* [2] who observed that within the same alloy the anomalous eutectic may have a dual origin. At relatively low undercoolings (~ 40 K) a fine-grained anomalous eutectic was formed which they concluded was due to the remelting of eutectic dendrites, while at high undercooling (~ 202 K) a coarse-grained anomalous eutectic was formed by partial remelting of single phase dendrites. However, there are relatively few systems in which eutectic

growth is reported to occur at such high undercoolings. Li & Zhou [9] suggested that such growth is probably restricted to systems in which at least one of the solidifying phases is an intermetallic, which would be the case for Ni-Sn, where the eutectic is formed between α-Ni and Ni_3Sn intermetallic. Consequently, the most likely origin for anomalous eutectic formation at low undercoolings, and certainly in alloys in which both eutectic phases are solid solutions, would seem to be partial remelting of eutectic dendrites.

In one study of Ag-Cu eutectic alloy it was suggested [10] that the formation of a cellular structure was possibly due to the large thermal diffusivity of the alloy melt and the large difference in the composition of the two phases, rather than due to the presence of an impurity element. This was further investigated in a study [6] looking at the effect of the inclusion of small amounts of Sb in Ag-Cu alloys. It was found that the addition of a third component caused a transition from cellular to dendritic structure at low undercoolings.

High speed video imaging is a useful technique that may be employed to investigate the solidification of undercooled melts and a number of alloys have been studied in this manner, including Ni-Ge [11], Ni-Si [12] and Ni-Sn [2] alloys. Normally, such imaging is performed on the whole droplet in order to monitor the rate at which the recalescence front progresses across the undercooled sample, wherein it is possible to estimate the solidification velocity. However, here we show that valuable additional information can be gained by monitoring the brightness as a function of time at spot locations on the sample surface.

Experimental Method

A high purity ingot of Ag-Cu alloy of eutectic composition was produced from 99.9999% purity (metals basis) silver and copper shot. The ingot was formed by sealing the metal shot in quartz tubing under a protective argon atmosphere and heating in a furnace to melt the silver and copper together whilst the tube was agitated to ensure thorough mixing. This procedure was repeated four times after which the quartz tube and resulting alloy were quenched in water. The ingot was sectioned and analysed using SEM and EDX to confirm it was homogenous and at the eutectic composition.

A melt fluxing technique was selected as the most suitable method with which to process Ag-Cu alloy. Samples of approximately 0.8 g of the Ag-Cu eutectic were cut from the ingot. Each sample was placed in a fused silica crucible measuring 10 mm in diameter by 20 mm long. In order to remove any microcracks from the inner surface of the crucibles, which could initiate nucleation, the crucibles were etched for 45 minutes in 7.2 vol.% HF solution and then rinsed thoroughly in distilled water followed by methanol prior to use. The crucible was packed with ground glass flux consisting of a 50:50 mixture of soda lime glass and boron oxide, this mixture giving the correct viscosity to fully encapsulate and support the alloy melt in the desired temperature range (from 300 K above to 100 K below the eutectic temperature). The molten flux supports the sample, isolating it from the solid surface of the crucible, and draws impurities and surface oxides away from the alloy melt, so inhibiting heterogeneous nucleation.

Undercooling experiments were performed within a stainless steel vacuum chamber evacuated to a pressure of 10^{-3} Pa using a turbo-molecular pump backed by a two stage, oil sealed, rotary vane pump. After being evacuated at this pressure for two hours the vacuum chamber was isolated from the pumping system by means of a gate valve and backfilled to 50 kPa with dry, oxygen free, N_2 gas. Samples were melted by induction heating of a graphite susceptor contained within an alumina shell. Viewing slots were cut into the susceptor and alumina to allow the sample to be viewed through a window in the chamber. Temperature determination was by means of a K-type thermocouple positioned beneath the crucible, which had been thinned at the base so reducing the thermal lag between the sample and thermocouple.

Prior to performing the undercooling experiments the B_2O_3 flux was dehydrated for one hour by heating to just below its melting point under high vacuum. The sample was then heated to 250-290 K above the eutectic temperature and held for 12 minutes before being allowed to cool to below

the eutectic temperature at the natural cooling rate of the apparatus, whereupon solidification would occur. This thermal cycling was repeated eight times for each alloy melt, allowing impurities to be removed from the sample and hence increasing the potential level of undercooling attainable. The process also has the desirable side-effect of removing any remaining bubbles from the flux so that the sample can be viewed clearly. On the final cycle the cooling and subsequent propagation of the recalescence front across the sample was recorded using a Photron Fastcam SA5 high speed camera. The camera was fitted with a Nikon AF Micro Nikkor 70-180 mm f/4.5-5.6D ED lens, allowing a clear view of the whole sample and a small amount of the surrounding flux to be obtained through a side observation port on the apparatus, with a working distance of 30 cm, as shown in Fig. 1. The experiment was repeated with multiple samples in order that a full range of undercooling could be investigated. Full details of the experimental apparatus are available elsewhere [13].
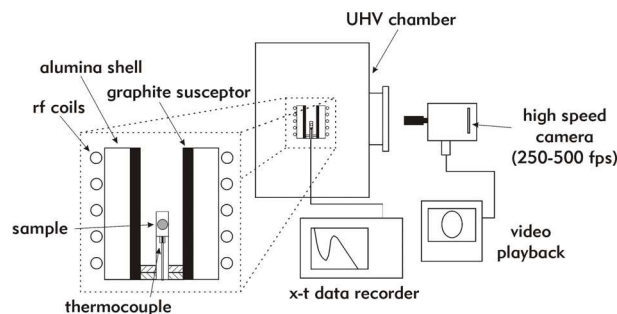

Fig. 1 Schematic view of the apparatus used to undercool Ag-Cu melt via flux encasement.

After removal from the flux each sample was mounted in Bakelite, sectioned, ground on a series of progressively finer SiC papers and then polished using 6 μm, 3 μm and 1 μm diamond compounds. Microstructural analysis of the as-solidified samples was undertaken using an XL30 ESEM and Carl Zeiss EVO® MA 15 SEM.

Results

Samples of eutectic Ag-Cu alloy were solidified from their parent melt, with the undercooling being increased from 0 in approximately 10 K steps. As reported by a number of sources [e.g 6, 14] the resulting microstructure for undercoolings below 70 K was found to be a mix of regular lamellar eutectic and anomalous eutectic, the volume fraction of the anomalous eutectic tending to increase with undercooling. The microstructure was generally found to be cellular, a typical cell consisting of lamellar eutectic in the body of the cell with anomalous eutectic occurring at the cell boundaries. Zones of different microstructure were also observed with an initial radial zone of anomalous eutectic followed by a cellular region of both lamellar and anomalous eutectic, as shown in Fig. 2. It appears that the development of the anomalous structure from the initial zone into the cellular zone was aligned with the growth direction, as determined by high speed imaging, and took the form of branched "fingers". No evidence of single phase dendrites is observed in the eutectic structures formed at $\Delta T = 60$ K, or below, whereas at 70 K and above extensive single phase dendrites are observed in the microstructure. The undercoolings for which anomalous eutectic structures were observed were $\Delta T = 10, 19, 27, 40, 51$ and 59 K.

Analysis of spot brightness on the sample has been performed by selecting a 7×7 pixel region of interest from the video, giving a spot size of ≈ 0.15 mm. From this analysis of spot brightness during recalescence two undercooling regimes can be identified. At low undercooling ($\Delta T \leq 19$ K), measurement of the spot brightness at different locations on the sample reveals two distinct types of recalescence behaviour. Near the nucleation zone (the region corresponding approximately to zone (a) in Fig. 2), there is a continuous increase in the spot brightness, which commences contemporaneously with nucleation. Conversely, further from the nucleation zone (the region corresponding approximately to zones (b & c) in Fig. 2) there is a rapid increase in the brightness as

the recalescence front passes the observation spot, with little prior indication that the front is approaching. These two types of behaviour are shown in Fig. 3a, for the sample undercooled by 19 K prior to nucleation. In this particular case the first (continuous) type of recalescence event has a peak grey level of 100, approximately 2 s after nucleation whereas the second type of recalescence event has a peak grey level of 182 with a rise time of 20 ms, after which there is a drop in the spot brightness followed by a second, more gradual recalescence event, detail of which is shown in Fig. 3b. This second recalescence is similar, both in shape and peak level, to that observed in the continuous recalescence zone. Although this is illustrated here from the sample undercooled by $\Delta T = 19$ K, similar results are observed at $\Delta T = 10$ K.
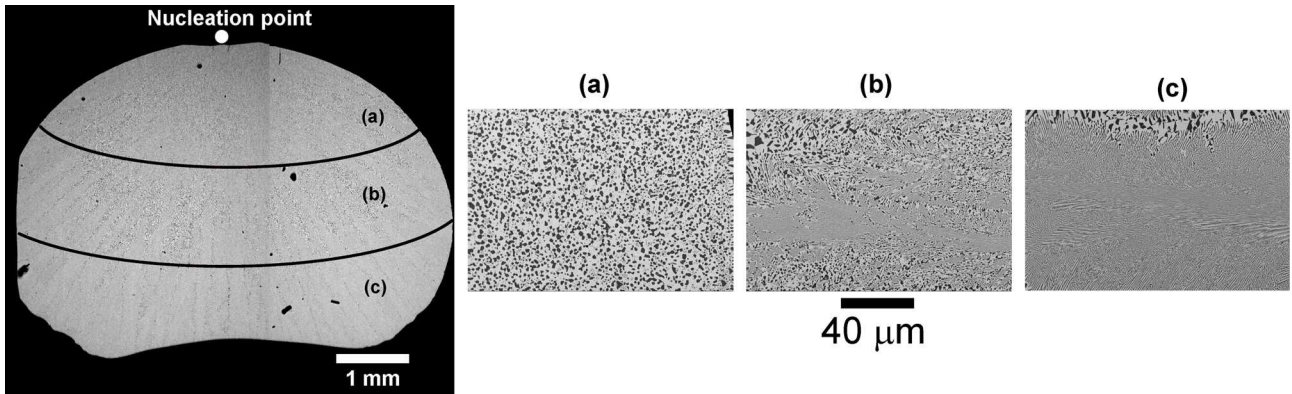

Fig. 2 Micrograph showing the variation of microstructure across an Ag-Cu alloy undercooled by 10 K. Outward radiating branched fingers of anomalous eutectic are clearly visible. To the right are shown typical example microstructures from the upper, middle and lower area of the sample, showing anomalous eutectic and very fine lamellar eutectic.

At higher undercoolings ($\Delta T \geq 27$ K) the sample does not display the continuous increase in spot brightness observed near the nucleation point at lower undercoolings, with only the second type of recalescence being observed at all locations on the sample. An example of this, obtained for the sample undercooled by 40 K prior to nucleation of solidification, is shown in Fig. 4. However, as before, broadly similar results are obtained at other undercoolings. The observation point on the sample was selected whereby solidification occurred approximately 1.5 s into the recalescence, which in total spans around 4.5 s. As for this type of recalescence when observed at $\Delta T = 19$ K, a rapid increase in the spot brightness is observed, followed by a steep decrease which we may associate with rapid local cooling and a subsequent, much more gentle second recalescence.
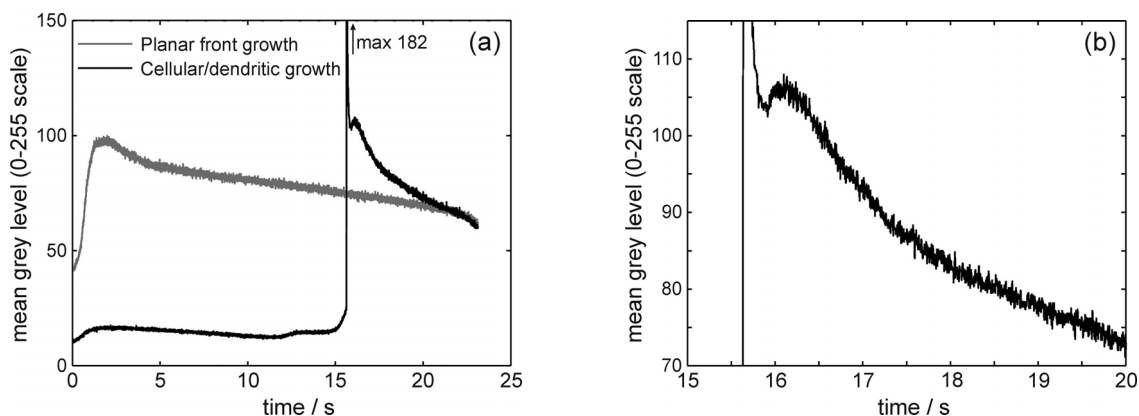

Fig. 3 (a) Spot brightness at two locations in the sample undercooled by $\Delta T = 19$ K illustrating the difference between planar and dendritic recalescence events and (b) detail of the second recalescence event following dendritic recalescence.
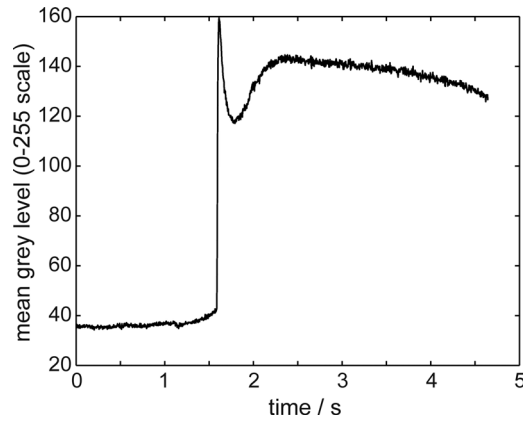
Fig. 4 Spot brightness (sample undercooled by $\Delta T = 40$ K) showing double recalescence.

Discussion and Conclusion

It is useful to classify these spot brightness profiles as being either 'planar' or 'dendritic' in character. During dendritic solidification the area behind the solidification front consists of a mush of dendritic crystals and the remaining interdendritic liquid, this latter acting as a heat sink for the latent heat released upon solidification. The volume fraction of the solid formed during the recalescence is therefore given, at least approximately, by $\Delta T c_p / L$, where c_p is the heat capacity and L the latent heat. Although there is a thermal field ahead of the solidification front, which will decay with a characteristic length scale of α/V (where α is the thermal diffusivity of the melt and V the velocity at which the solidification front advances), the continued propagation of the front does not rely upon the undercooled liquid ahead of the front acting as a sink for latent heat. Conversely, during the propagation of a planar front, as would be the case with a lamellar eutectic, the area behind the solidification front will be fully solid and the continued propagation of the front relies upon either continued heat extraction through the solid or the undercooled liquid ahead of the front acting as a sink for the evolved latent heat. The growth of a planar eutectic into an undercooled melt is therefore normally regarded as being a non-steady-state process, with the continued evolution of latent heat during growth resulting in a slowing of growth with time.

Referring to Fig. 3a, the shape of the brightness-time curves would strongly suggest that for the continuous type recalescence we are observing the propagation of a planar (eutectic) growth front. The gradual increase in brightness prior to the maximum being observed would then be ascribed to the approach of the planar eutectic front and its preceding thermal profile. In this case, the peak in the grey level 2 s after nucleation would represent the planar front crossing the observation point, and the grey level observed here would correspond to the local temperature of the eutectic interface. Conversely, the near step change in brightness observed during the second type of recalescence event would be much more likely to be indicative of a dendritic, or non-space filling recalescence, in which a mush was formed behind the advancing solidification front. However, it is not possible to determine from the video data whether this is due to the growth of cells or dendrites. In all cases we note that following the initial rapid increase in brightness there is a drop in brightness, followed by a second, more gradual recalescence event. This second recalescence is similar to that observed during continuous recalescence and may therefore correspond to the planar front growth of a lamellar eutectic growing into the residual liquid following primary recalescence.

However, noting the very significant difference in peak brightness between the primary and secondary recalescence events, this would also suggest that the primary recalescence was to a temperature in excess of the eutectic temperature, which would be consistent with the anomalous eutectic in the as-solidified samples being formed by partial remelting of primary single or two-phase cells/dendrites. Moreover, as the liquidus temperature for the two solid-solutions will be different, recalescence to a temperature between these two would only melt one of these phases and coarsen the other.

We therefore surmise that at moderate to high undercooling initial recalescence is the result of the growth of a non space-filling morphology, the most likely of which we consider to be two-phase (eutectic) cells or dendrites, with the subsequent planar front growth of lamellar eutectic filling the interdendritic regions. Within such a solidification sequence remelting of eutectic cells or dendrites is the most likely origin of the anomalous eutectic. This would appear to be supported by the observation that the first recalescence event is significantly brighter than the second, implying that there may be local heating above the eutectic temperature to facilitate remelting. Planar front growth does not occur until considerable post-recalescence cooling has taken place. An origin for the anomalous eutectic in which it was formed by remelting of eutectic dendrites during the rapid solidification phase of growth with subsequent solidification of the interdendritic liquid to a planar eutectic would also be consistent with the observation of many workers that the volume fraction of the anomalous structure increases with undercooling.

References

[1] T. Z. Kattamis and M. C. Flemings, Structure of undercooled Ni-Sn eutectic, Metall. Trans. 1 (1970) 1449.

[2] C. Yang, J. Gao, Y. K. Zhang, M. Kolbe, and D. M. Herlach, New evidence for the dual origin of anomalous eutectic structures in undercooled Ni-Sn alloys: In situ observations and EBSD characterization, Acta Mater. 59 (2011) 3915.

[3] R. Goetzinger, M. Barth, D. M. Herlach, Mechanism of formation of the anomalous eutectic structure in rapidly solidified Ni-Si, Co-Sb and Ni-Al-Ti alloys, Acta Mater. 46 (1998) 1647.

[4] M. Li and K. Kuribayashi, Nucleation-controlled microstructures and anomalous eutectic formation in undercooled Co-Sn and Ni-Si eutectic melts, Metall. Mater. Trans. A 34 (2003) 2999.

[5] N. Wang, C. D. Cao, B. Wei, Solidification behaviour of silver-copper alloys in a drop tube, Adv. Space Res. 24 (1999) 1257.

[6] S. Zhao, J. F. Li, L. Liu, and Y. H. Zhou, Solidification of undercooled Ag-Cu eutectic alloy with the Sb addition, J. Alloys and Comp. 478 (2009) 252.

[7] B. Wei, D. M. Herlach, F. Sommer, and W. Kurz, Rapid dendritic and eutectic solidification of undercooled Co-Mo alloys, Mater. Sci. Eng. A181/A182 (1994) 1150.

[8] S. Zhao, J. F. Li, L. Liu, and Y. H. Zhou, Eutectic growth from cellular to dendritic form in the undercooled Ag-Cu eutectic alloy melt, J. Cryst. Growth 311 (2009) 1387.

[9] J. F. Li and Y. H. Zhou, Eutectic growth in bulk undercooled melts, Acta Mater. 53 (2005) 2351.

[10] S. Zhao, J. F. Li, L. Liu, and Y. H. Zhou, Cellular growth of lamellar eutectics in undercooled Ag-Cu alloy, Mater. Charact. 60 (2009) 519.

[11] R. Ahmad, R. F. Cochrane and A. M. Mullis, Disorder trapping during the solidification of βNi_3Ge from its deeply undercooled melt, J. Mater. Sci. 47 (2012) 2411.

[12] R. Ahmad, R. F. Cochrane and A. M. Mullis, The formation of regular αNi-γ ($Ni_{31}Si_{12}$) eutectic structures from undercooled Ni-25 at.% Si melts, Intermetallics 22 (2012) 55.

[13] S. E. Battersby, R. F. Cochrane and A. M. Mullis, Highly undercooled germanium: Growth velocity measurements and microstructural analysis, Mater. Sci. Eng. A 226 (1997) 443.

[14] C. R. Clopet, R. F. Cochrane and A. M. Mullis, Spasmodic growth during the rapid solidification of undercooled Ag-Cu eutectic melts, Appl. Phys. Lett. 102 (2013) 031906.